



Structural basis for intramolecular interaction of post-translationally modified H-Ras.GTP prepared by protein ligation

Ke, Haoliang ; Matsumoto, Shigeyuki ; Murashima, Yosuke ; Taniguchi-Tamura, Haruka ; Miyamoto, Ryo ; Yoshikawa, Yoko ; Tsuda, Chiemi ;...

(Citation)

FEBS Letters, 591(16):2470-2481

(Issue Date)

2017-08

(Resource Type)

journal article

(Version)

Accepted Manuscript

(Rights)

©2017 Federation of European Biochemical Societies. This is the peer reviewed version of the following article: [FEBS Letters, 591(16):2470-2481, 2017], which has been published in final form at <http://dx.doi.org/10.1002/1873-3468.12759>. This article may be used for non-commercial purposes in accordance with Wiley Terms and Conditions fo...

(URL)

<https://hdl.handle.net/20.500.14094/90004244>



Title: Structural basis for intramolecular interaction of posttranslationally modified H-Ras•GTP prepared by protein ligation

Author names: Haoliang Ke^{a, 1}, Shigeyuki Matsumoto^{a, 1}, Yosuke Murashima^a, Haruka Taniguchi-Tamura^a, Ryo Miyamoto^a, Yoko Yoshikawa^a, Chiemi Tsuda^a, Takashi Kumasaka^b, Eiichi Mizohata^c, Hironori Edamatsu^a, and Tohru Kataoka^{a,*}

Affiliations:

^aDivision of Molecular Biology, Department of Biochemistry and Molecular Biology, Kobe University Graduate School of Medicine, 7-5-1 Kusunoki-cho, Chuo-ku, Kobe 650-0017, Japan

^bJapan Synchrotron Radiation Research Institute (JASRI), 1-1-1 Kouto, Sayo-cho, Sayo-gun, Hyogo 679-5198, Japan

^cDepartment of Applied Chemistry, Graduate School of Engineering, Osaka University, 2-1 Yamadaoka, Suita, Osaka 565-0871, Japan

¹These authors contributed equally to this work.

*Corresponding author: Tohru Kataoka

Address: Division of Molecular Biology, Department of Biochemistry and Molecular Biology, Kobe University Graduate School of Medicine, 7-5-1 Kusunoki-cho, Chuo-ku, Kobe 650-0017, Japan
Telephone: +81-78-382-5380; Fax: +81-78-382-5399; e-mail: kataoka@people.kobe-u.ac.jp

Abstract

Ras undergoes posttranslational modifications including farnesylation, proteolysis and carboxymethylation at the C terminus, which are necessary for membrane recruitment and effector recognition. Full activation of c-Raf-1 requires cooperative interaction of the farnesylated C terminus and the activator region of Ras with its cysteine-rich domain (CRD). However, molecular basis for this interaction remains unclear because of difficulties in preparing modified Ras sufficient for structural studies. Here we use Sortase A-catalyzed protein ligation to prepare modified Ras sufficient for NMR and X-ray crystallographic analyses. The results show that the farnesylated C terminus establishes an intramolecular interaction with the catalytic domain and brings the farnesyl moiety to the proximity of the activator region, which may be responsible for their cooperative recognition of c-Raf-1-CRD.

Keywords: Ras, farnesylation, protein structure

Abbreviations: GEF, guanine nucleotide exchange factor; Sos, Son of Sevenless; PI3K, phosphoinositide 3-kinase; GAP, GTPase-activating protein; HVR, hypervariable region; RBD, Ras-binding domain; CRD, cysteine-rich domain; SrtA, Sortase A; GST, glutathione-S-transferase; Ab, antibody; DTT, dithiothreitol; GppNHp, guanosine 5'-(β,γ -imido)triphosphate; n-OG, n-Octyl- β -D-glucoside; MALDI-TOF-MS, matrix-assisted laser desorption ionization time of flight

mass spectrometry; SPR, surface plasmon resonance; HSQC, heteronuclear single-quantum coherence; rms, root mean square.

Introduction

Small GTPases H-Ras, K-Ras and N-Ras, collectively called Ras, are the products of the *ras* proto-oncogenes and function as a molecular switch for controlling cell proliferation, differentiation and survival by interconverting between the GDP-bound “OFF” and GTP-bound “ON” forms (Ras•GDP and Ras•GTP, respectively) [1]. In response to the extracellular stimuli, Ras•GTP is generated from Ras•GDP through the catalysis by guanine nucleotide exchange factors (GEFs) such as Son of Sevenless (Sos) and interacts directly with various effector proteins, such as Raf kinases (c-Raf-1, B-Raf and A-Raf), phosphoinositide 3-kinases (PI3Ks), Ral-GEFs and phospholipase C α , leading to activation of the respective downstream signaling pathways. On the other hand, the intrinsic GTPase activity is responsible for conversion of Ras•GTP to Ras•GDP, which is accelerated by GTPase-activating proteins (GAPs). Ras protein is grossly divided into two parts: the catalytic domain (Ras¹⁻¹⁶⁶) corresponding to the amino acid residues 1-166 and the hypervariable region (HVR) corresponding to the residues 167-189 in H-Ras, K-Ras4A and N-Ras (Fig. S1A). Ras¹⁻¹⁶⁶, whose amino acid sequence is highly conserved among the isoforms, harbors the guanine nucleotides and, in its GTP-bound form, associates with the Ras-binding domains (RBDs) of the effectors through its flexible binding interface composed of two regions, Switch I (residues 32-38) and Switch II (residues 60-75) [2-5]. In addition, the residues 23-31 and 39-50 flanking Switch I are named the “activator region” because they contain various substitutions in a Ras-homologue Rap1, which has an antagonistic effect toward Ras-dependent malignant transformation, and because introduction of Rap1-type substitutions into this region indeed abrogated the activity to activate c-Raf-1 [6-8]. On the other hand, the amino acid sequence of HVR is highly divergent except for the C-terminal CAAX motif (A, aliphatic amino acids; X, any amino acids), which is subjected to a series of posttranslational modification reactions as follows [9]. As the first step, a farnesyl group is covalently attached to Cys186 in the CAAX motif by farnesyltransferase. This prenylation reaction is followed by proteolytic removal of the AAX tripeptide by Ras-converting enzyme-1 and subsequently by carboxymethylation of the resulting C-terminal Cys by isoprenylcysteine carboxymethyltransferase-1. These modifications are essential for recruitment of Ras to the plasma membrane. In addition, a further modification step, where a palmitoyl group is attached to the Cys residues immediately upstream of the CAAX motif by palmitoyltransferase, stabilizes the membrane anchoring of farnesylated H-Ras, N-Ras and K-Ras4A. We showed that the posttranslational modifications, especially the farnesylation, of Ras, are necessary for the full activation of the effectors such as c-Raf-1 and yeast adenylyl cyclase [10, 11]. The N-terminal regulatory region of c-Raf-1 contains two domains responsible for the interaction with Ras, RBD (residues 51-131) and the cysteine-rich domain (CRD, residues 139-184) [12] (Fig. S1A). RBD binds to the residues in Switch I with the K_D value of 10^{-7} ~ 10^{-8} M order in a GTP-dependent manner, whose molecular basis was clarified by X-ray crystallography [3, 13, 14]. On the other hand, CRD

binds to Ras in a manner independent of the nature of the guanine nucleotide, and this interaction is necessary for the full activation of c-Raf-1 [11, 15-18]. We showed that the Ras-CRD interaction is dependent on the farnesylation of H-Ras and abolished by substitutions, such as N26G and V45E, in the activator region, suggesting that the farnesylated C terminus and the activator region might cooperatively recognize CRD [15]. However, the molecular basis for this interaction remains elusive because of the difficulties in preparing posttranslationally modified Ras in an amount sufficient for structural studies by NMR and X-ray crystallography. In the present study, to address this problem, we make use of a protein ligation reaction catalyzed by a transpeptidase from *Staphylococcus aureus*, Sortase A (SrtA). SrtA cleaves a peptide bond between Thr and Gly in a recognition motif LPXTG attached to the donor (poly)peptides and executes a transpeptidation reaction between the resulting carboxyl group of Thr and an amino group of the N-terminal Gly attached to the acceptor (poly)peptides [19, 20] (Fig. S1B). Accordingly, we are able to prepare H-Ras carrying various degrees of the modifications in amounts sufficient for structural studies by ligating between H-Ras¹⁻¹⁶⁶, attached with LPXTG, and the synthetic HVR peptides, attached with Gly and carrying chemical modifications equal to those in the cells (Table 1). This procedure enables us to introduce stable isotope labeling into the residues 1-166 for structural analysis using NMR, and the results show that HVR makes an intramolecular interaction with a region of the catalytic domain encompassing the C terminus to the activator region across the central β sheet and that this interaction brings the farnesyl moiety to the vicinity of the activator region, which may be responsible for their cooperative recognition of c-Raf-1-CRD. Furthermore, we are able to solve the crystal structure of modified H-Ras for the first time, showing that the existence of modified HVR induces conformational changes of the α 2-helix in Switch II, the C terminus of the α 3-helix and the following loop. Since these regions were shown to be involved in the effector recognition, structural interconversion in the GTP-bound form and the intrinsic GTP-hydrolyzing activity [4, 21-23], the result suggests that the postranslational modifications may exert more global influence on the cellular function of Ras than previously thought.

Materials and methods

Plasmids: pFLAG-CMV2-H-Ras, an expression vector of FLAG-tagged full-length H-Ras, was described before [24]. pFLAG-CMV2-H-Ras(LPKTG), where the residues 167-171 of H-Ras was replaced by LPTKG, was constructed by oligonucleotide-directed mutagenesis using In-Fusion HD Cloning System (Clontech Laboratories). pGEX-6P-1-H-Ras and pQE-30 Xa-H-Ras were used for expression of H-Ras¹⁻¹⁶⁶ as a glutathione-S-transferase (GST) fusion and with a 6 \times His tag, respectively, in *Escherichia coli* (*E. coli*) [25]. pGEX-6P-1-H-Ras^{substrate} expressing GST-fusion H-Ras¹⁻¹⁶⁶ attached with LPKTG and a 6 \times His tag at its C terminus was constructed by oligonucleotide-directed mutagenesis. pET28A-SSORA d59, an *E. coli* expression vector for SrtA attached with a C-terminal 6 \times His tag, was kindly provided by Dr. Tomohiko Yamazaki (Research Center for Functional Materials, National Institute for Materials Science, Tsukuba, Japan).

Antibodies: Rabbit anti-MEK (#9122), rabbit anti-phospho-MEK(Ser217/221) (#9121) and rabbit

anti-FLAG tag (#2368) antibodies (Abs) were obtained from Cell Signaling Technologies. Rabbit anti-H-Ras C20 Ab (SC-520), raised against the C-terminal 20 residues of H-Ras, was obtained from Santa Cruz Biotechnology. Goat anti-rabbit IgG Ab was obtained from GE Healthcare.

Synthetic HVR peptides: Peptides with various degrees of the modifications, which correspond to the residues 172 to the C termini of H-Ras, carry amino acid substitutions of Ser for Cys181 and Cys184 and are added with the SrtA recognition signal Gly at their N termini (Table 1), were synthesized and obtained from Peptide Institute, Inc. (Osaka, Japan). The authenticity of the peptides was confirmed by mass spectrometric analyses.

Cell culture and transfection: Human embryonic kidney AD293 cells were cultured in Dulbecco's modified Eagle's medium supplemented with 10% fetal bovine serum, penicillin and streptomycin, and transfected with the expression vectors using Lipofectamine 2000 (Thermo-Fisher Scientific). In 20-24 h after transfection, cells were lysed in 50 mM Tris-HCl, pH 7.4, 150 mM NaCl, 1 mM EDTA, 1 mM dithiothreitol (DTT), phosphatase inhibitor cocktail (Nacalai Tesque, Kyoto, Japan) and protease inhibitor cocktail (Nacalai Tesque), and, after centrifugation at $1,000 \times g$ for 20 min, the resulting supernatant was subjected to Western blotting. Protein concentration was determined by Quick Start Bradford Reagent (BIO-RAD).

Western blotting: Proteins were separated by standard SDS-PAGE and transferred onto PVDF membranes. The membrane was probed by an appropriate primary antibody, followed by a horse radish peroxidase-conjugated goat anti-rabbit IgG Ab. The immunoreactive signals were developed with ImmunoStar Zerta (Wako Pure Chemicals, Japan) and detected by using ImageQuant LAS 4000 mini (GE Healthcare).

Protein production and purification: *E. coli* BL21 (DE3) cells harboring pGEX-6P-1-H-Ras, pGEX-6P-1-H-Ras^{substrate}, pQE-30 Xa-H-Ras or pET28A-SSORA d59 were grown at 18 °C in the presence of 0.15 mM isopropyl β -D-1-thiogalactopyranoside for 18 h for production of the respective recombinant proteins. Uniform labeling of H-Ras¹⁻¹⁶⁶ and H-Ras^{substrate} with ¹⁵N and ¹³C was performed as described before [23]. The cells were disrupted by sonication in buffer A (50 mM Tris-HCl, pH 8.0, 1 mM EDTA, 150 mM NaCl, 10 mM MgCl₂, 1 mM DTT and 0.01% Triton X-100) and, after centrifugation at $30,000 \times g$ for 20 min, GST-fusion H-Ras¹⁻¹⁶⁶ and H-Ras^{substrate} were purified from the resulting supernatant by absorption onto glutathione-Sepharose 4B resin (GE Healthcare) and elution by on-column cleavage with Turbo3C protease (Accelagen, California, USA) [23]. 6 \times His-tagged H-Ras¹⁻¹⁶⁶ was purified by absorption onto Ni-NTA resin (QIAGEN) and elution with 100 mM imidazole. The eluted Ras proteins were further purified by HiTrap Q HP column chromatography (GE Healthcare) and subsequently loaded with a non-hydrolyzable GTP analogue, guanosine 5'-(β , γ -imido) triphosphate (GppNHp) [25].

Production of H-Ras•GppNHp carrying various degrees of the modifications: SrtA and H-Ras^{substrate} produced in *E. coli* were separately immobilized on Ni-NTA agarose resin (QIAGEN). Subsequently, the SrtA-immobilized resin, the H-Ras^{substrate}-immobilized resin and the synthetic HVR peptides were mixed together at the protein/peptide molar ratio of 1:8:10 and incubated at 30 °C for 24

h in the presence of 500 μ M GDP and 20 mM CaCl_2 . The resulting ligation products were then eluted by washing the resin with buffer A, loaded with GppNHp and immobilized on glutathione-Sepharose 4B resin. After washing with 50 mM Tris-HCl, pH 8.0, 150 mM NaCl, 10 mM MgCl_2 , 1 mM DTT and 3.4 mM n-Octyl- β -D-glucoside (n-OG), H-Ras was eluted by cleavage with Turbo3C protease.

Mass spectrometric analyses: The ligation products were analyzed by matrix-assisted laser desorption ionization time of flight mass spectrometry (MALDI-TOF-MS). After desalting and removal of detergent by using ZipTip_{SCX} (Millipore), 2.5 μ l of the sample solution was co-crystallized with matrix (20 mg/ml 2, 5-dihydroxybenzoic acid in 30% acetonitrile and 0.1% trifluoroacetic acid) on a target plate at room temperature, and the spectra were acquired on a Bruker UltraFlex III instrument in the linear positive mode. The calibration was done by using Protein standard II (Bruker Daltonics).

Surface plasmon resonance (SPR) analysis: Binding of the HVR peptides to H-Ras¹⁻¹⁶⁶ was measured by using Biacore T200 (GE Healthcare). 6 \times His-tagged H-Ras¹⁻¹⁶⁶•GppNHp was immobilized on an NTA sensor chip to the density of approximately 2,500 RU. The HVR peptides were introduced at 25 °C with a flow rate of 30 μ l/min in a running buffer (10 mM HEPES, pH 7.4, 150 mM NaCl, 0.05 mM EDTA and 0.05% Tween-20) with a contact time of 2 min. The difference in the sensorgram between the blank flow cell and the protein-immobilized flow cell was used for the binding analysis.

NMR spectroscopy: NMR spectra were recorded on a Bruker AVANCE III 600 instrument equipped with shielded gradient triple-resonance probes in NMR measurement buffer (25 mM phosphate buffer, pH 6.8, 50 mM NaCl, 10 mM MgCl_2 , 1 mM DTT and 3.4 mM n-OG) containing 10% (v/v) D_2O at 298 K and analyzed by using NMRPipe [26] and NMRView (One Moon Scientific, New Jersey, USA). The backbone signal assignment of H-Ras^{substrate} was carried out with a series of three dimensional spectra for sequential assignment procedures, HNCACB, CBCACONH, HNCA, HN(CO)CA, HNCO and HNCACO, on 0.5 mM $^{13}\text{C}/^{15}\text{N}$ -labeled sample. The backbone signal assignments of the ligation products and H-Ras¹⁻¹⁶⁶ were achieved by utilizing the data on H-Ras^{substrate} and our previous data [27], respectively. The measurement of ^1H - ^{15}N HSQC spectra was carried out on 40 μ M Ras, and 1.6 mM of the HVR peptides were mixed with H-Ras¹⁻¹⁶⁶ for the binding experiments. The chemical shift perturbations were calculated as $\Delta\delta_{NH} = \sqrt{(\Delta\delta_H)^2 + (\Delta\delta_N/5)^2}$, where $\Delta\delta_H$ and $\Delta\delta_N$ are the changes in the chemical shift values for ^1H and ^{15}N , respectively.

Crystallization of modified H-Ras•GppNHp and X-ray structure determination: A single crystal of modified H-Ras•GppNHp was obtained by the hanging drop vapor diffusion method at 20 °C with 1 μ l of 12.7 mg/mL protein solution mixed with 1 μ l of a reservoir solution [0.1 M 2-(N-morpholino)ethanesulfonic acid, pH 6.0, 0.1 M $\text{Ca}(\text{OAc})_2$ and 20% (w/v) polyethylene glycol 8000]. A microseeding technique successfully allowed to grow the crystal further. The crystal was flash-cooled to 100 K with a nitrogen cryostream using the reservoir solution containing 20% (v/v) glycerol as a cryoprotectant. X-ray diffraction data were collected at SPring-8 BL38B1. Diffraction data processing and scaling were performed using the HKL-2000 package [28]. The crystal structure

was solved by the molecular replacement method using the program Molrep [29] with the coordinate of H-Ras¹⁻¹⁶⁶•GppNHp (PDB code 3K8Y) as a search model. The structural refinement and the interactive rebuilding process were carried out by the programs Refmac [30] and Coot [31], respectively. Data collection and refinement statistics are listed in Table 2. The R_{sym} value became slightly high depending on the quality of the crystal. The atomic coordinate has been deposited in the Protein Data Bank (PDB; <http://www.rcsb.org>) under the accession code 5X9S.

Results

In vitro production of H-Ras proteins carrying various degrees of the modifications

HVR of H-Ras contains three Cys residues: Cys181 and Cys184 to be palmitoylated and Cys186 to be farnesylated. Because of the technical difficulty in attachment of a farnesyl group to the genuine HVR peptide, we decided to replace Cys181 and Cys184 by Ser in the HVR peptides and disregard the effect of palmitoylation in the present study. Accordingly, we produced four kinds of H-Ras proteins representing various stages of the posttranslational modifications except for the palmitoylation: H-Ras^{CVLS}, H-Ras^{C(Far)VLS}, H-Ras^{C(Far)} and H-Ras^{C(Far)OMe}, by the SrtA-catalyzed ligation of bacterially expressed H-Ras^{substrate} with the corresponding synthetic HVR peptides (Table 1). Optimization study of the reaction condition showed that the highest yield of the ligation products was obtained when the reaction was carried out at 30 °C for 24 h at the molecular ratio of 1:8:10 for H-Ras^{substrate}, SrtA and HVR peptides. Typically, 0.3 mg of H-Ras^{C(Far)OMe}•GppNHp was obtained from 24 mg of H-Ras^{substrate} and 4.4 mg of the C(Far)OMe peptide. Each of the ligation products exhibited a single major band in SDS-PAGE (Fig. 1A) and could be detected by anti-H-Ras C20 Ab (Fig. 1B), indicating the completion of the ligation reaction. Moreover, when the purified H-Ras^{CVLS}, H-Ras^{C(Far)VLS}, H-Ras^{C(Far)} and H-Ras^{C(Far)OMe} were subjected to MALDI-TOF-MS analysis, the estimated molecular masses of their major components matched well with those predicted from their chemical formulas. In the ligation products, the residues 167-171 of HVR were replaced by LPTKG. To examine the effect of this replacement on the cellular activity, we expressed H-Ras and H-Ras(LPKTG), both carrying an activating mutation G12V to get rid of the influence of upstream regulatory factors, in AD293 cells and observed no detectable difference in the ability to induce MEK activation (Fig. 1C). These results strongly suggested that the ligation products were the functional equivalents of the genuine H-Ras proteins.

NMR analyses for the intramolecular interaction between the catalytic domain and HVR and effect of the posttranslational modifications

To investigate the effect of the attachment of the unmodified and modified HVR on the structure of the catalytic domain by NMR, H-Ras^{CVLS} and H-Ras^{C(Far)OMe} were prepared by ligating uniformly ¹⁵N-labeled H-Ras^{substrate} with the corresponding HVR peptides, loaded with GppNHp and subjected to the measurements of ¹H-¹⁵N HSQC spectra, which were simplified due to the absence of the NH signals arising from the HVR residues. The spectra of both H-Ras^{CVLS}•GppNHp and H-Ras^{C(Far)OMe}•GppNHp displayed well-dispersed cross-peaks, indicating that the proteins were stably

folded (Fig. S2A and B). Signal assignments for the two proteins were achieved with reference to the data on H-Ras^{substrate}•GppNHp in which 136 residues out of 163 non-Pro residues were assigned. Unassigned residues with severely broadened signals were mainly located in the regions including Switch I and Switch II, which underwent interconversion between two conformational states on a millisecond time scale [32]. Spectral comparison between H-Ras^{CVLS}•GppNHp and H-Ras^{substrate}•GppNHp revealed that a number of signals exhibited significant chemical shift perturbations and that their corresponding residues were mainly located in the region encompassing the C terminus (Ile163-Gln165) to the activator region (His27, Val44, Val45 and Glu49) across the central β sheet (Thr2, Lys5 and Leu6 in the β 1-strand and Cys51-Leu53 in the β 3-strand) (Fig. 2A, B and E), suggesting that the unmodified HVR established an intramolecular interaction with these regions of the catalytic domain. The ^1H - ^{15}N HSQC spectrum of H-Ras^{C(Far)OMe}•GppNHp exhibited similar signal changes to those of H-Ras^{CVLS}•GppNHp (Fig. 2C). However, it showed additional chemical shift perturbations or severe signal broadening for the residues located in the activator region and its proximity, Phe28, Asp54 and Ile55, suggesting that the modified HVR carrying the farnesyl group was positioned in proximity to the distal part of the activator region (Figs. 2A, 2D, E and S3). Among the residues exhibiting the signal changes in the ^1H - ^{15}N HSQC spectra of H-Ras^{CVLS}•GppNHp and H-Ras^{C(Far)OMe}•GppNHp, Val8, Gly77, Phe78, Leu79, Phe156 and Val160 were buried in the hydrophobic core (Fig. 2E). Therefore, it was likely that they were incapable of establishing any contacts with HVR and that the observed signal changes were attributed to either a secondary effect of the conformational change in the neighboring residues or the changes in their own conformational dynamics, or both of them.

To further prove the interaction of HVR with the catalytic domain, we analyzed the binding of the C(Far)OMe HVR peptide to H-Ras¹⁻¹⁶⁶•GppNHp by ^1H - ^{15}N HSQC experiments. The result showed that Tyr40 in the activator region and the solvent-exposed residues, Ala66, Gln70, and Thr74, in the α 2-helix exhibited significant chemical shift perturbations (Fig. 3). Taken together, these results strongly suggested that the farnesyl moiety is positioned in the proximity of the activator region via the intramolecular interaction between HVR and the catalytic domain. Consistent with the NMR data, SPR analyses showed that the CFarOMe HVR peptide exhibited dose-dependent binding to H-Ras¹⁻¹⁶⁶•GppNHp at the concentrations ranging from 0.5 to 2.0 mM (Fig. S4). The observed response values seemed too high considering the molecular weight of the CFarOMe HVR peptide, however, this could be accounted for by association of a Tween-20 micelle with the peptide in the running buffer. The CVLS HVR peptide showed weaker binding barely detectable at the concentration of 4 mM, indicating that the modifications had a facilitative effect on the interaction.

Crystal structure of modified H-Ras and its structural differences from unmodified H-Ras

We successfully determined the crystal structure of H-Ras^{C(Far)OMe}•GppNHp for the first time at the resolution of 2.5 Å. No electron density corresponding to the modified HVR was observed, suggesting that its structure was heavily disordered. Data collection and refinement statistics are listed in Table 2. The overall structure of the catalytic domain was similar to that of H-Ras¹⁻¹⁶⁶•GppNHp (PDB code

3K8Y). Superimposition of the two structures indicated that a large part of the α 2-helix in Switch II was unstructured and that the C-terminal part of the α 3-helix and the following loop were shifted toward the α 2-helix (Fig. 4A and B). These regions were known to adopt variable conformations with functional relevance as found in the active and inactive states of Ras•GTP and the complexes with Sos and PI3K γ [4, 22] (Fig. 4C, see Discussion). The conformational changes agreed well with the NMR data in that the residues in the corresponding region: Ala66, Met67, Arg68, Thr74 and Gly75 in the α 2-helix and Lys104 in the α 3-helix, showed significant signal changes in ^1H - ^{15}N HSQC spectrum of H-Ras^{C(Far)OMe}•GppNHp (Fig. 2C and E) although we cannot exclude the possibility that they were contributed by the crystal packing effect. In the crystal structure, Val8, Gly77, Phe78, Leu79 and Val81, which exhibited the HSQC signal perturbations despite their location in the hydrophobic core, were found to be located adjacent to the regions showing the conformational changes, proving that their HSQC signal changes were likely to be ascribable to the secondary effect of the conformational changes in the neighboring regions.

Discussion

Although Ras proteins exert their cellular functions as the posttranslationally modified form, their structural studies had been regularly carried out using the unmodified form often truncated with HVR. One of its major reasons was the problem of tremendous difficulties in preparation of modified Ras in an amount sufficient for structural studies by NMR and X-ray crystallography. In the present study, we addressed this problem by the adoption of the SrtA-catalyzed protein ligation. Moreover, the method enabled us to systematically produce modified Ras proteins representing various stages of the posttranslational modifications and to introduce stable isotope labeling into the catalytic domain for NMR analysis. Actually, the SrtA-catalyzed ligation reaction had been employed to produce a similar of modified K-Ras4B, however, a sulfo-SMCC crosslinking agent was used to attach the farnesylated and carboxymethylated Cys to the C terminus and the product was not functionally characterized in detail [33]. Recently, Gillette *et al.* reported high yield production of fully modified K-Ras4B using an improved insect cell expression system, which will certainly facilitate the structural study on modified Ras [34]. By comparison, our method has the advantage of making possible the analysis of the role of the individual modification steps and the labeling of the products by stable isotopes or other means.

In this study, we have demonstrated the existence of an intramolecular interaction of the modified HVR with the catalytic domain of H-Ras•GppNHp and clarified its molecular basis by comparison of the NMR spectra among H-Ras^{substrate}•GppNHp, H-Ras^{CVLS}•GppNHp and H-Ras^{C(Far)OMe}•GppNHp and of the crystal structures between H-Ras¹⁻¹⁶⁶•GppNHp and H-Ras^{C(Far)OMe}•GppNHp. Moreover, the interaction was further supported by the binding experiment of the C(Far)OMe HVR peptide to the catalytic domain by using NMR and SPR. The results showed that HVR interacts intramolecularly with a region of the catalytic domain encompassing the C terminus to the activator region across the central β sheet and that this causes positioning of the modified HVR carrying the farnesyl group in proximity to the distal part of the activator region. The observations that a millimolar concentration of

the C(Far)OMe HVR peptide was required for the detection of its binding to H-Ras¹⁻¹⁶⁶•GppNHp in both NMR and SPR and that the modified HVR was completely disordered in the crystal structure of H-Ras^{C(Far)OMe}•GppNHp suggest the low-affinity and transient nature of their intramolecular interaction, although the low affinity observed for the peptide-protein binding could be compensated to some extent by the covalent attachment of HVR to the C terminus of the catalytic domain. The functional significance of this low-affinity intramolecular interaction remains to be clarified further, particularly with regard to how it is compatible with the interaction of the farnesyl moiety with membrane lipids and trafficking/scaffolding proteins such as PDE δ and Galectin [35-38]. Also, the SPR analyses showed that the posttranslational modifications strengthened the binding of the HVR peptide to H-Ras¹⁻¹⁶⁶•GppNHp (Fig. S4), suggesting that they might stabilize the intramolecular interaction. These results supported the notion by Thaper *et al.* [39] suggesting the existence of a weak interaction between the farnesyl moiety and the hydrophobic residues on the activator region, Phe28 and Val29, as one interpretation for their NMR data. In the case of K-Ras4B, the interaction of the unmodified HVR with the catalytic domain had been observed, which seemed to be mediated by an electrostatic interaction contributed by the polybasic region of HVR [40]. It must be noted that the protein ligation resulted in the replacement of the residues 167-171 in HVR with LPTKG. Thaper *et al.* [39] had reported that the region encompassing these residues was intrinsically unstable but exhibited a propensity for adopting an α -helical structure, raising a possibility that the replacement might alter the flexibility of HVR thereby affecting its intramolecular interaction with H-Ras¹⁻¹⁶⁶. Although we cannot fully exclude this possibility, the absence of the effect on the cellular activity of Ras to activate c-Raf-1 (Fig. 1C) implies that the replacement is unlikely to have a significant effect on the structure and function of Ras.

The molecular mechanism for the cellular activation of c-Raf-1 by modified Ras•GTP involves complex processes including membrane recruitment, phosphorylations, protein-protein interactions including dimerization and resulting conformational changes, the whole picture of which still remains to be clarified [41]. Previous studies had indicated that Ras directly binds to c-Raf-1-CRD and that this interaction is necessary for the full activation of c-Raf-1 and dependent on the farnesylation and the activator region of Ras [11, 15-18], suggesting that the farnesylated C terminus and the activator region might cooperatively recognize CRD. Consistent with this, an NMR study using H-Ras•GDP, which was modified by *in vitro* farnesylation but lacked the AAX removal and the carboxymethylation, had suggested the existence of an interaction with c-Raf-1-CRD through the residues 23-32 in the activator region and the residues 183-189 in the farnesylated HVR of H-Ras [39]. Our present results suggested that H-Ras^{C(Far)OMe}•GppNHp might adopt a compact tertiary structure where the farnesylated HVR is arranged in close proximity to the activator region, which may form a molecular basis for their cooperative binding to CRD (Fig. S5). The farnesyl moiety might contribute to a hydrophobic interaction between Ras and CRD and, in that case, the carboxymethylation of Cys186 might serve to strengthen this interaction as observed for the interaction between farnesylated K-Ras4B and PDE δ , where the binding affinity became approximately two orders of magnitude higher depending on the

carboxymethylation [42]. In this line, biochemical and structural characterization of H-Ras^{C(Far)VLS} and H-Ras^{C(Far)} may provide further insight into the significance of the carboxymethylation as well as the AAX removal. The functional significance of the Ras-c-Raf-1-CRD interaction remains to be clarified further, particularly with regard to how it is compatible with the interaction of the farnesyl moiety with membrane lipids and trafficking/scaffolding proteins such as PDE δ and Galectin [35-38]. The role of the farnesyl moiety in the plasma membrane localization would be compensated by the palmitoylation in H-Ras, N-Ras and K-Ras4A and by the polybasic region in K-Ras4B.

The crystal structure of H-Ras^{C(Far)OMe}•GppNHp revealed that the α 2- and α 3-helices adopted local structures distinct from those of H-Ras¹⁻¹⁶⁶•GppNHp. Because the α 2- and α 3-helices are known to undergo diverse conformational changes in association with a wide range of the physiological functions, such as the recognition of the effector molecules, the intrinsic GTP hydrolysis and the structural interconversion between the inactive and active states of Ras•GTP [4, 21-23] (Fig. 4C), the posttranslational modifications may significantly affect the biophysical and biochemical parameters of Ras proteins relevant to their cellular functions. Since such parameters have regularly been determined using unmodified Ras often truncated with HVR, they must be critically examined using the posttranslationally modified form.

Acknowledgements

The synchrotron radiation experiments were performed at BL38B1 in SPring-8 with the approval of Japan Synchrotron Radiation Research Institute (JASRI) (Proposal No. 2016A2515). We thank Drs. Seiki Baba and Takashi Kawamura of JASRI/SPring-8 for data collection and helpful advices. We also thank Dr. Tomohiko Yamazaki of Research Center for Functional Materials, National Institute for Materials Science (Tsukuba, Japan) for kindly donating pET28A-SSORA d59. The SPR experiments were supported by Center for Medical Research and Education, Graduate School of Medicine, Osaka University (Osaka, Japan). This work was supported by JSPS KAKENHI Grant Number 26293065.

Author contributions

TKA conceived and supervised the study; SM, HE and TKA designed experiments; HK, SM, YM, HT, RM, YY, CT, TKU and EM performed experiments; HK, SM, YM, HT, RM, YY, TKU and HE analyzed data; SM and TKA wrote the manuscript; SM and TKA made manuscript revisions.

References

1. Karnoub, A. E. and Weinberg, R. A. (2008) Ras oncogenes: split personalities. *Nat. Rev. Mol. Cell. Biol.* 9, 517-531.
2. Huang, L., Hofer, F., Martin, G. S. and Kim, S. H. (1998) Structural basis for the interaction of Ras with RalGDS. *Nat. Struct. Biol.* 5, 422-426.
3. Nassar, N., Horn, G., Herrmann, C., Scherer, A., McCormick, F. and Wittinghofer, A. (1995) The 2.2 Å crystal structure of the Ras-binding domain of the serine/threonine kinase c-Raf1 in complex

with Rap1A and a GTP analogue. *Nature* 375, 554-560.

4. Pacold, M. E., Suire, S., Perisic, O., Lara-Gonzalez, S., Davis, C. T., Walker, E. H., Hawkins, P. T., Stephens, L., Eccleston, J. F. and Williams, R. L. (2000) Crystal structure and functional analysis of Ras binding to its effector phosphoinositide 3-kinase γ . *Cell* 103, 931-943.
5. Vetter, I. R. and Wittinghofer, A. (2001) The guanine nucleotide-binding switch in three dimensions. *Science* 294, 1299-1304.
6. Shirouzu, M., Koide, H., Fujita-Yoshigaki, J., Oshio, H., Toyama, Y., Yamasaki, K., Fuhrman, S. A., Villafranca, E., Kaziro, Y. & Yokoyama, S. (1994) Mutations that abolish the ability of Ha-Ras to associate with Raf-1. *Oncogene*. 9, 2153-2157.
7. Kitayama, H., Sugimoto, Y., Matsuzaki, T., Ikawa, Y. and Noda, M. (1989) A ras-related gene with transformation suppressor activity. *Cell*. 56, 77-84.
8. Marshall, M. S. (1993) The effector interactions of p21ras. *Trends Biochem. Sci.* 18, 250-254.
9. Konstantinopoulos, P. A., Karamouzis, M. V. and Papavassiliou, A. G. (2007) Post-translational modifications and regulation of the RAS superfamily of GTPases as anticancer targets. *Nat. Rev. Drug Discov.* 6, 541-555.
10. Kuroda, Y., Suzuki, N. and Kataoka, T. (1993) The effect of posttranslational modifications on the interaction of Ras2 with adenylyl cyclase. *Science* 259, 683-686.
11. Tamada, M., Hu, C. D., Kariya, K., Okada, T. and Kataoka, T. (1997) Membrane recruitment of Raf-1 is not the only function of Ras in Raf-1 activation. *Oncogene* 15, 2959-2964.
12. Daum, G., Eisenmann-Tappe, I., Fries, H. W., Troppmair, J. and Rapp, U. R. (1994) The ins and outs of Raf kinases. *Trends Biochem. Sci.* 19, 474-480.
13. Fetis, S. K., Guterres, H., Kearney, B. M., Buhman, G., Ma, B., Nussinov, R. and Mattos, C. (2015) Allosteric effects of the oncogenic RasQ61L mutant on Raf-RBD. *Structure* 23, 505-516.
14. Herrmann, C., Martin, G. A. and Wittinghofer, A. (1995) Quantitative analysis of the complex between p21ras and the Ras-binding domain of the human Raf-1 protein kinase. *J. Biol. Chem.* 270, 2901-2905.
15. Hu, C. D., Kariya, K., Tamada, M., Akasaka, K., Shirouzu, M., Yokoyama, S. and Kataoka, T. (1995) Cysteine-rich region of Raf-1 interacts with activator domain of post-translationally modified Ha-Ras. *J. Biol. Chem.* 270, 30274-30277.
16. Luo, Z., Diaz, B., Marshall, M. S. and Avruch, J. (1997) An intact Raf zinc finger is required for optimal binding to processed Ras and for ras-dependent Raf activation in situ. *Mol. Cell. Biol.* 17, 46-53.
17. Mineo, C., Anderson, R. G. and White, M. A. (1997) Physical association with ras enhances activation of membrane-bound raf (RafCAAX). *J. Biol. Chem.* 272, 10345-10348.
18. Roy, S., Lane, A., Yan, J., McPherson, R. and Hancock, J. F. (1997) Activity of plasma membrane-recruited Raf-1 is regulated by Ras via the Raf zinc finger. *J. Biol. Chem.* 272, 20139-20145.
19. Kobashigawa, Y., Kumeta, H., Ogura, K. and Inagaki, F. (2009) Attachment of an NMR-invisible

- solubility enhancement tag using a sortase-mediated protein ligation method. *J. Biomol. NMR* 43, 145-150.
20. Mao, H., Hart, S. A., Schink, A. and Pollok, B. A. (2004) Sortase-mediated protein ligation: a new method for protein engineering. *J. Am. Chem. Soc.* 126, 2670-2671.
 21. Buhrman, G., Holzapfel, G., Fetics, S. and Mattos, C. (2010) Allosteric modulation of Ras positions Q61 for a direct role in catalysis. *Proc. Natl. Acad. Sci. USA* 107, 4931-4936.
 22. Margarit, S. M., Sondermann, H., Hall, B. E., Nagar, B., Hoelz, A., Pirruccello, M., Bar-Sagi, D. and Kuriyan, J. (2003) Structural evidence for feedback activation by Ras•GTP of the Ras-specific nucleotide exchange factor SOS. *Cell* 112, 685-695.
 23. Matsumoto, S., Miyano, N., Baba, S., Liao, J., Kawamura, T., Tsuda, C., Takeda, A., Yamamoto, M., Kumasaka, T., Kataoka, T. and Shima, F. (2016) Molecular mechanism for conformational dynamics of Ras•GTP elucidated from in-situ structural transition in crystal. *Sci. Rep.* 6, 25931.
 24. Nomura, K., Kanemura, H., Satoh, T. and Kataoka, T. (2004) Identification of a novel domain of Ras and Rap1 that directs their differential subcellular localizations. *J. Biol. Chem.* 279, 22664-22673.
 25. Liao, J., Shima, F., Araki, M., Ye, M., Muraoka, S., Sugimoto, T., Kawamura, M., Yamamoto, N., Tamura, A. and Kataoka, T. (2008) Two conformational states of Ras GTPase exhibit differential GTP-binding kinetics. *Biochem. Biophys. Res. Comm.* 369, 327-332.
 26. Delaglio, F., Grzesiek, S., Vuister, G. W., Zhu, G., Pfeifer, J. and Bax, A. (1995) NMRPipe: a multidimensional spectral processing system based on UNIX pipes. *J. Biomol. NMR* 6, 277-293.
 27. Araki, M., Shima, F., Yoshikawa, Y., Muraoka, S., Ijiri, Y., Nagahara, Y., Shirono, T., Kataoka, T. and Tamura, A. (2011) Solution structure of the state 1 conformer of GTP-bound H-Ras protein and distinct dynamic properties between the state 1 and state 2 conformers. *J. Biol. Chem.* 286, 39644-39653.
 28. Otwinowski, Z. and Minor, W. (1997) Processing of X-ray diffraction data collected in oscillation mode. *Method. Enzymol.* 276, 307-326.
 29. Vagin, A. and Teplyakov, A. (1997) MOLREP: an automated program for molecular replacement. *J. Appl. Crystallogr.* 30, 1022-1025.
 30. Murshudov, G. N., Skubak, P., Lebedev, A. A., Pannu, N. S., Steiner, R. A., Nicholls, R. A., Winn, M. D., Long, F. and Vagin, A. A. (2011) REFMAC5 for the refinement of macromolecular crystal structures. *Acta Crystallogr. D* 67, 355-367.
 31. Emsley, P. and Cowtan, K. (2004) Coot: model-building tools for molecular graphics. *Acta Crystallogr. D* 60, 2126-2132.
 32. Geyer, M., Schweins, T., Herrmann, C., Prisner, T., Wittinghofer, A. and Kalbitzer, H. R. (1996) Conformational transitions in p21ras and in its complexes with the effector protein Raf-RBD and the GTPase activating protein GAP. *Biochemistry* 35, 10308-10320.
 33. Dementiev, A. (2012) K-Ras4B lipoprotein synthesis: biochemical characterization, functional properties, and dimer formation. *Protein Expr. Purif.* 84, 86-93.

34. Gillette, W. K., Esposito, D., Abreu Blanco, M., Alexander, P., Bindu, L., Bittner, C., Chertov, O., Frank, P. H., Grose, C., Jones, J. E., Meng, Z., Perkins, S., Van, Q., Ghirlando, R., Fivash, M., Nissley, D. V., McCormick, F., Holderfield, M. and Stephen, A. G. (2015) Farnesylated and methylated KRAS4b: high yield production of protein suitable for biophysical studies of prenylated protein-lipid interactions. *Sci. Rep.* 5, 15916.
35. Elad-Sfadia, G., Haklai, R., Balan, E. & Kloog, Y. (2004) Galectin-3 augments K-Ras activation and triggers a Ras signal that attenuates ERK but not phosphoinositide 3-kinase activity, *The Journal of biological chemistry.* 279, 34922-30.
36. Hanzal-Bayer, M., Renault, L., Roversi, P., Wittinghofer, A. & Hillig, R. C. (2002) The complex of Arl2-GTP and PDE delta: from structure to function, *The EMBO journal.* 21, 2095-106.
37. Nancy, V., Callebaut, I., El Marjou, A. & de Gunzburg, J. (2002) The delta subunit of retinal rod cGMP phosphodiesterase regulates the membrane association of Ras and Rap GTPases, *The Journal of biological chemistry.* 277, 15076-84.
38. Paz, A., Haklai, R., Elad-Sfadia, G., Ballan, E. & Kloog, Y. (2001) Galectin-1 binds oncogenic H-Ras to mediate Ras membrane anchorage and cell transformation, *Oncogene.* 20, 7486-93.
39. Thapar, R., Williams, J. G. and Campbell, S. L. (2004) NMR characterization of full-length farnesylated and non-farnesylated H-Ras and its implications for Raf activation. *J. Mol. Biol.* 343, 1391-1408.
40. Chavan, T. S., Jang, H., Khavrutskii, L., Abraham, S. J., Banerjee, A., Freed, B. C., Johannessen, L., Tarasov, S. G., Gaponenko, V., Nussinov, R. and Tarasova, N. I. (2015) High-affinity interaction of the K-Ras4B hypervariable region with the Ras active site. *Biophys. J.* 109, 2602-2613.
41. Roskoski, R., Jr. (2010) RAF protein-serine/threonine kinases: structure and regulation. *Biochem. Biophys. Res. Comm.* 399, 313-317.
42. Dharmiah, S., Bindu, L., Tran, T. H., Gillette, W. K., Frank, P. H., Ghirlando, R., Nissley, D. V., Esposito, D., McCormick, F., Stephen, A. G. and Simanshu, D. K. (2016) Structural basis of recognition of farnesylated and methylated KRAS4b by PDEδ. *Proc. Natl. Acad. Sci. USA* 113, 6766-6775.
43. Kabsch, W. and Sander, C. (1983) Dictionary of protein secondary structure: pattern recognition of hydrogen-bonded and geometrical features, *Biopolymers* 22, 2577-2637.

Figure legends

Fig. 1. Characterization of H-Ras carrying various degrees of the modifications. (A) The purified ligation products: H-Ras^{CVLS}, H-Ras^{C(Far)VLS}, H-Ras^{C(Far)} and H-Ras^{C(Far)OMe}, H-Ras¹⁻¹⁶⁶ and H-Ras^{substrate}. were separated by SDS-PAGE (15% gel) and stained with Coomassie Brilliant Blue. M: molecular size markers. (B) The purified ligation products were subjected to Western blotting using anti-H-Ras C20 Ab. (C) AD293 cells were transfected with either pFLAG-CMV2-H-RasG12V(LPKTG) [G12V(LPKTG)], pFLAG-CMV2-H-RasG12V (G12V), pFLAG-CMV2-H-Ras (WT) or pFLAG-CMV2 (Vector), and the lysate of the cells was fractionated by SDS-PAGE (15% gel) and

subjected to Western blotting using anti-phospho-MEK (pMEK), anti-MEK (tMEK) and anti-FLAG tag (FLAG) Abs.

Fig. 2. NH signal changes of the catalytic domain residues depending on the attachment of the unmodified and modified HVR. (A) The ^1H - ^{15}N HSQC spectra of representative residues exhibiting significant NH signal changes are shown: H-Ras^{substrate}•GppNHp (black), H-Ras^{CVLS}•GppNHp (red) and H-Ras^{C(Far)OMe}•GppNHp (green). (B) Chemical shift perturbations of the NH signals between H-Ras^{CVLS}•GppNHp and H-Ras^{substrate}•GppNHp are shown for the individual residues in the catalytic domain. The red horizontal line indicates the sum of the average and the standard deviation. A diagram representing the secondary structure of H-Ras¹⁻¹⁶⁶•GppNHp (PDB code 3K8Y) is shown at the bottom, where α -helices and β -strands are indicated by red rectangles and blue arrows, respectively. (C) Chemical shift perturbations between H-Ras^{C(Far)OMe}•GppNHp and H-Ras^{substrate}•GppNHp are shown similarly as (B). The signals of Asp54, Ala66 and Met67 were excluded from the analyses because they exhibited severe broadening in the presence of the posttranslational modifications (Fig. S3). (D) Chemical shift perturbations between H-Ras^{CVLS}•GppNHp and H-Ras^{C(Far)OMe}•GppNHp are shown similarly as (B). (E) The residues exhibiting significant NH signal changes in H-Ras^{CVLS}•GppNHp are shown in a red color on the tertiary structure of H-Ras¹⁻¹⁶⁶•GppNHp (PDB code 3K8Y). The C α atoms of the residues showing additional signal changes between H-Ras^{CVLS}•GppNHp and H-Ras^{C(Far)OMe}•GppNHp are shown by spheres. Unassigned residues and residues excluded from the analysis because of signal overlapping and broadening in the ^1H - ^{15}N HSQC spectrum of H-Ras^{substrate}•GppNHp are shown in a black color. GppNHp is shown in the stick model.

Fig. 3. NH signal changes of the catalytic domain residues of H-Ras¹⁻¹⁶⁶•GppNHp depending on the addition of the modified HVR peptide. (A) Chemical shift perturbations induced by the addition of the C(Far)OMe HVR peptide are shown for the individual residues in the catalytic domain. The red horizontal line indicates the sum of the average and the standard deviation. The secondary structure diagram is identical with that of Fig. 2B. (B) The residues exhibiting significant NH signal changes are shown in a red color on the tertiary structure of H-Ras¹⁻¹⁶⁶•GppNHp (PDB code 3K8Y). Unassigned residues and residues excluded from the analysis because of signal overlapping and broadening in the ^1H - ^{15}N HSQC spectrum of H-Ras¹⁻¹⁶⁶•GppNHp are shown in a black color. GppNHp is shown in the stick model.

Fig. 4. Comparison of the crystal structures among H-Ras^{C(Far)OMe}•GppNHp and various forms of H-Ras¹⁻¹⁶⁶•GppNHp. (A) The crystal structures of H-Ras¹⁻¹⁶⁶•GppNHp (colored in green) and H-Ras^{C(Far)OMe}•GppNHp (colored in light gray) are superimposed using the C α atoms of the residues 1-31, 39-59 and 76-166. The secondary structure assignments were achieved with the DSSP algorithm [43]. (B) The distances of the C α atoms in the superimposed structures are plotted for the individual residues in the catalytic domain. The α 2-helix, the C-terminal part of the α 3-helix and the following

loop are highlighted by a yellow color. The secondary structure diagram is identical with that of Fig. 2B. (C) The crystal structure of H-Ras¹⁻¹⁶⁶•GppNHp in complex with Sos (yellow, PDB code 1NVW), that in complex with PI3K γ (magenta, PDB code 1HE8) and that of the GTP-bound inactive state known as “state 1” (blue, PDB code 5B30) were superimposed with the crystal structure of H-Ras^{C(Far)OMe}•GppNHp (light gray). The superimposition was carried out by using the C α atoms of the residues 1-31, 39-59 and 76-166.

Table 1. Amino acid sequences of the synthetic HVR peptides used in this study.

Peptides	Amino acid sequences	Molecular size (Da)
CVLS	G-NPPDESGPGSMSSKCVLS	1849
C(Far)VLS	G-NPPDESGPGSMSSKC(Far) ^a VLS	2053.4
C(Far)	G-NPPDESGPGSMSSKC(Far)	1754
C(Far)OMe	G-NPPDESGPGSMSSKC(Far)OCH ₃ ^b	1768

^a (Far) indicates a farnesyl moiety attached to Cys186.

^b OCH₃ indicates that Cys186 is carboxymethylated.

Table 2. Data collection and refinement statistics.

PDB ID	5X9S
Data collection	
X-ray source	SPRing-8 BL38B1
Detector	Rayonix MX225 HE
Wavelength (Å)	1.000
Space group	<i>H</i> 32
Cell dimensions	
a, b, c (Å)	88.47, 88.47, 134.05
α , β , γ (°)	90, 90, 120
Resolution (Å)	50.0–2.50 (2.54–2.50) ^a
No. observed reflections	77203
No. unique reflections	7216
R_{sym} (%) ^b	0.159 (0.490)
I/σ_I	21.6 (6.4)
Completeness (%)	100.0 (100.0)
Redundancy	10.7 (11.0)
$CC_{1/2}$	0.99 (0.95)
Refinement	
Resolution (Å)	36.83–2.50
No. reflections	7220
$R_{\text{work}}/R_{\text{free}}$ ^c	0.183/0.236
R.m.s. deviations	
Bond lengths (Å)	0.0082
Bond angles (°)	1.3
Ramachandran outliers/favored (%)	0/96.3
Clashscore, all atoms	2

A single crystal was used for each data collection and structure refinement.

^aValues in parentheses are for highest-resolution shell.

^b $R_{\text{sym}} = \sum_{hkl} \sum_j |I_{hkl,j} - I_{hkl}| / \sum_{hkl} \sum_j I_{hkl,j}$, where I_{hkl} is the average of symmetry-related observations of a unique reflection.

^c $R_{\text{work}} = \sum_{hkl} ||F_{\text{obs}}(hkl)| - |F_{\text{calc}}(hkl)|| / \sum_{hkl} |F_{\text{obs}}(hkl)|$. R_{free} = the cross-validation R factor for 5% of reflections against which the model was not refined.

Figure 1

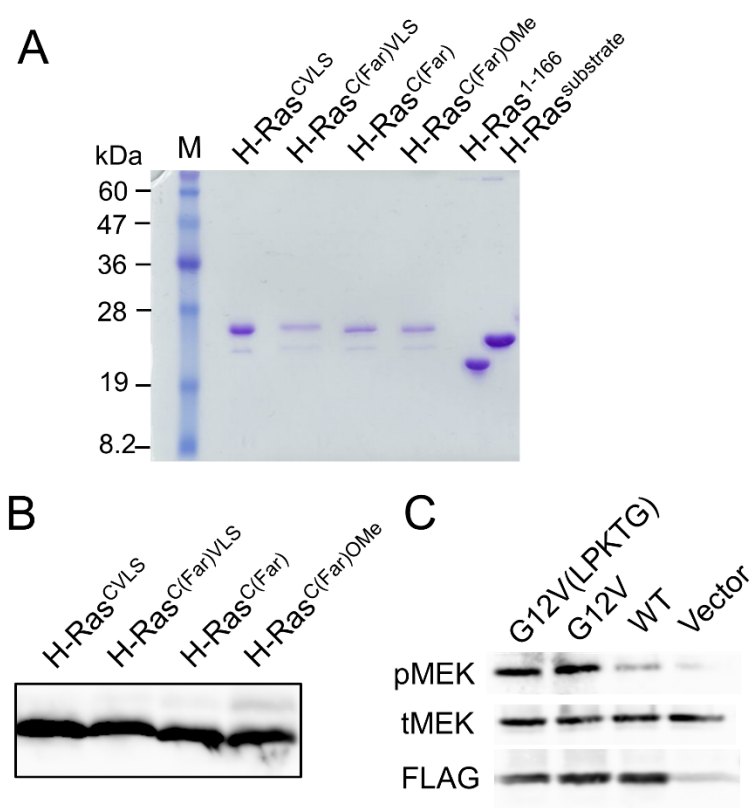


Figure 2

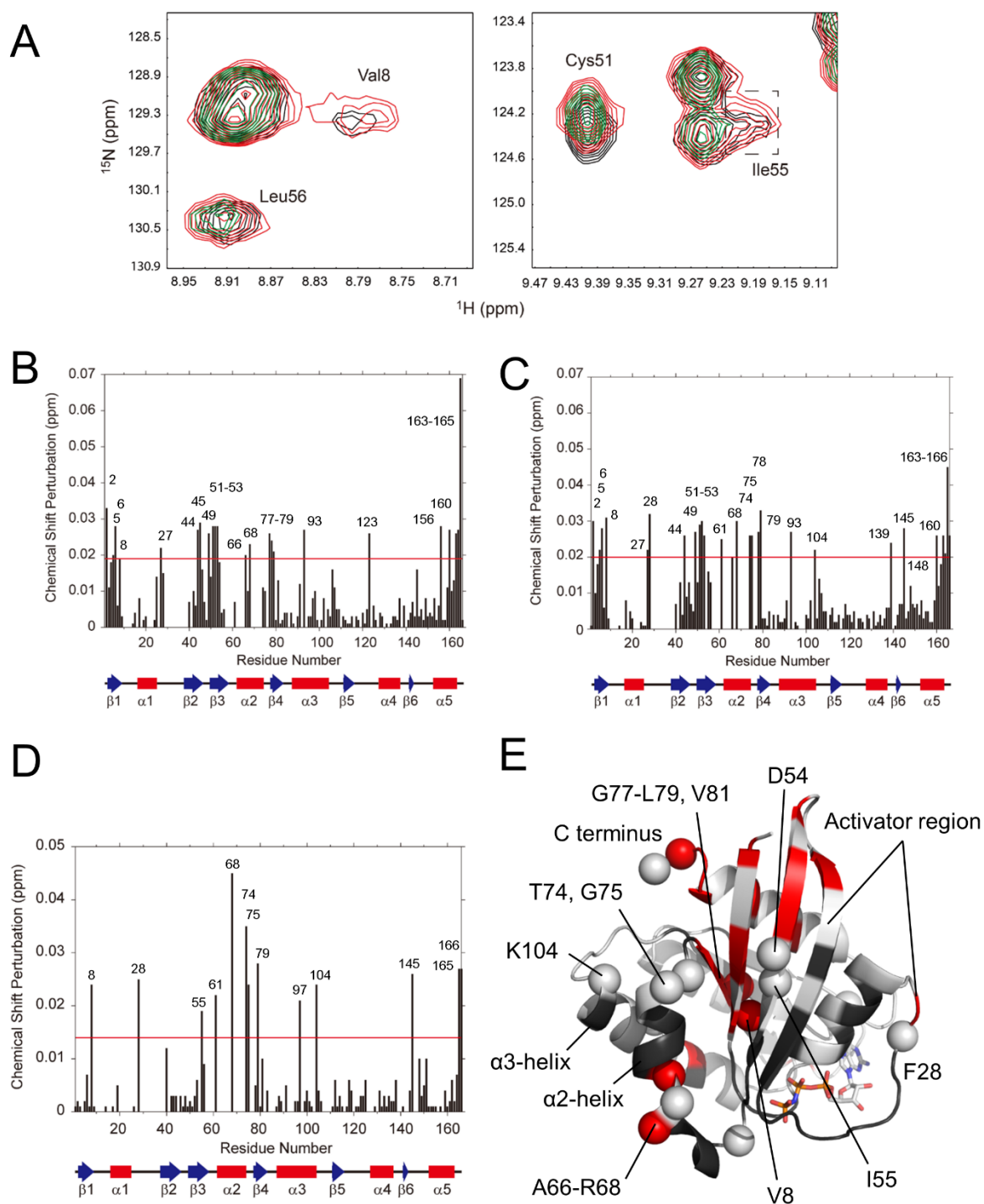


Figure 3

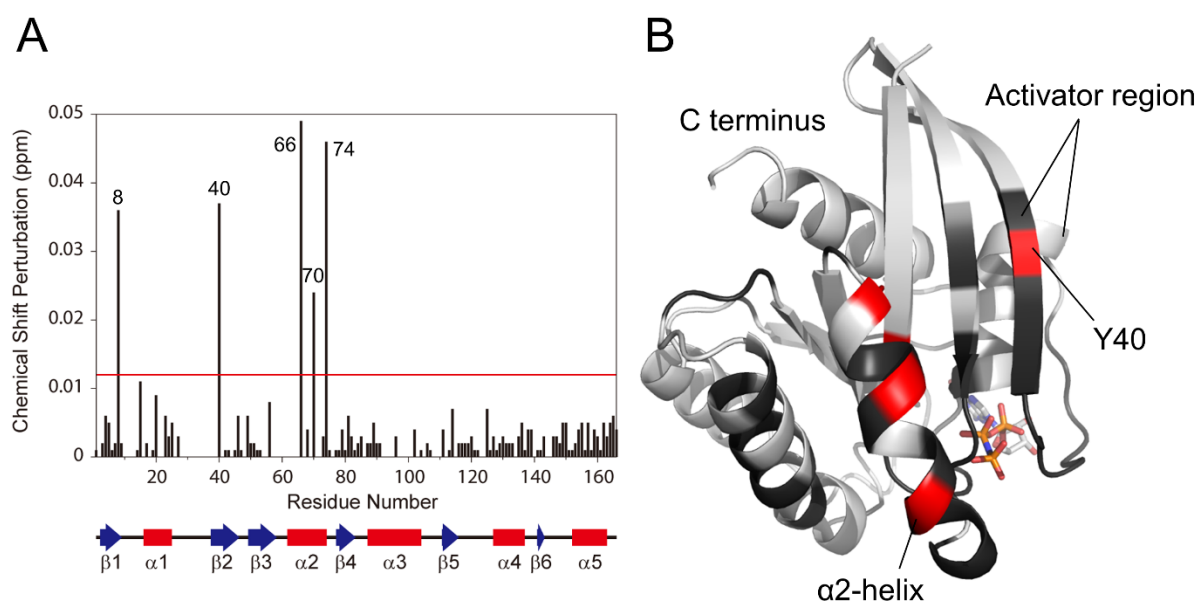
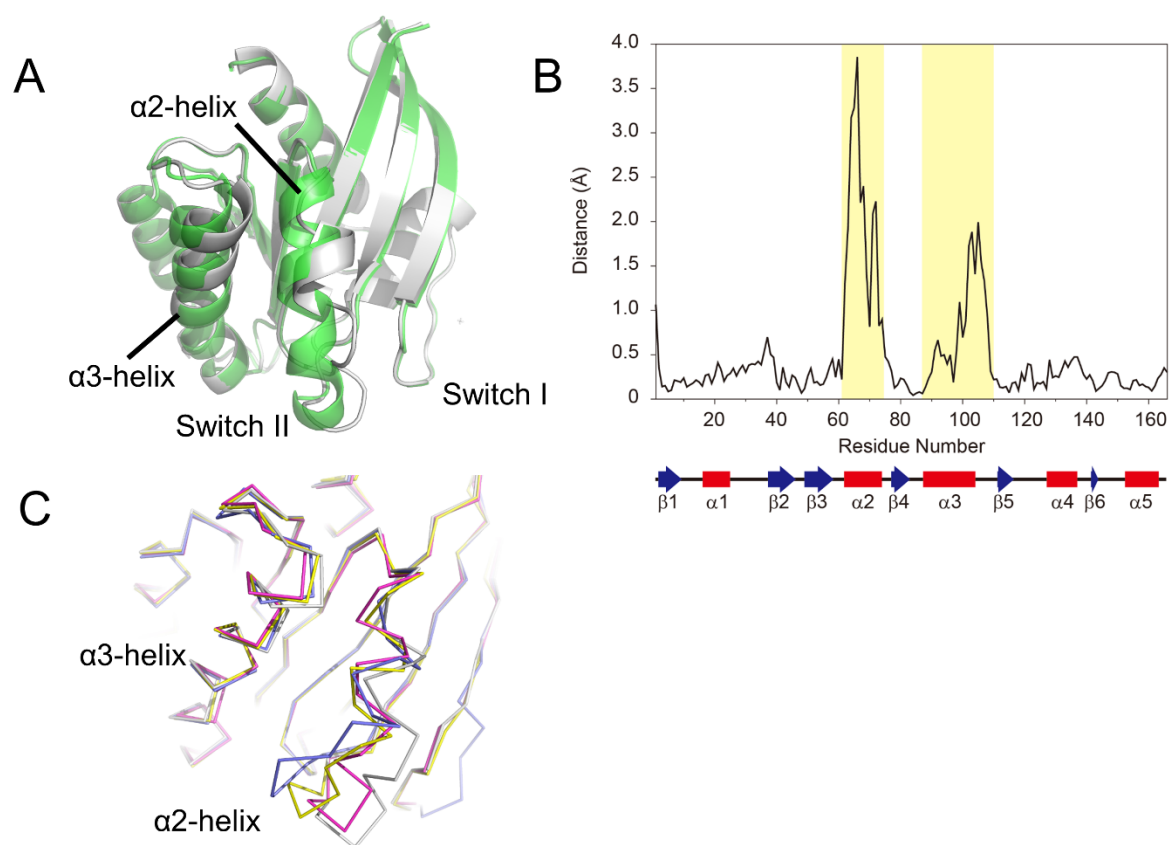


Figure 4



Supporting Information

Fig. S1. Domain structures of H-Ras and c-Raf-1 and schematic representation of the SrtA-catalyzed transpeptidation reaction. (A) Switch I, Switch II, the activator region and posttranslationally modified HVR of H-Ras and RBD and CRD of c-Raf-1 are colored by yellow, green, dark gray, light gray, magenta and cyan, respectively. The numbers above the bars indicate the residue numbers demarcating the various domains. Far represents the farnesyl moiety. (B) The SrtA-recognition motifs, LPXTG attached to the donor H-Ras¹⁻¹⁶⁶ and Gly attached to the acceptor HVR peptide, are shown.

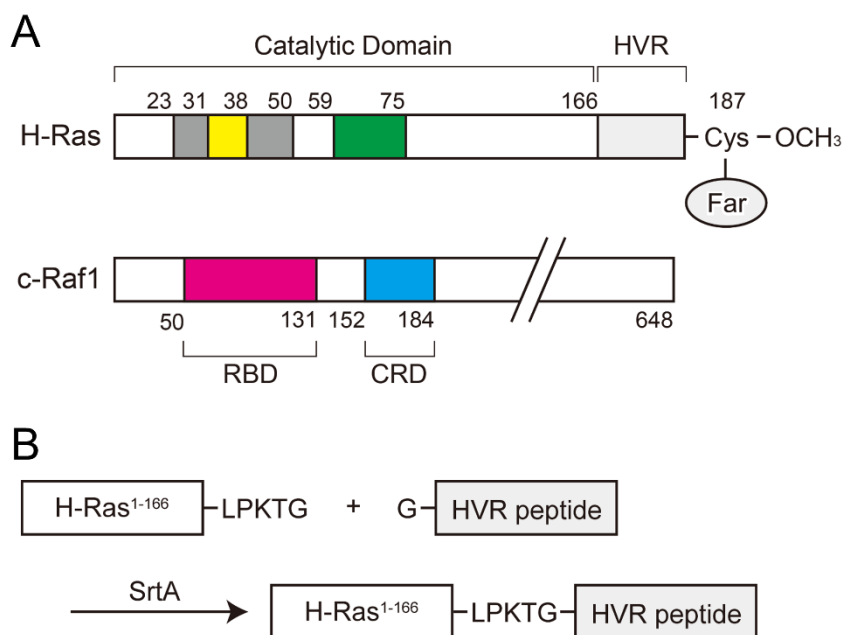
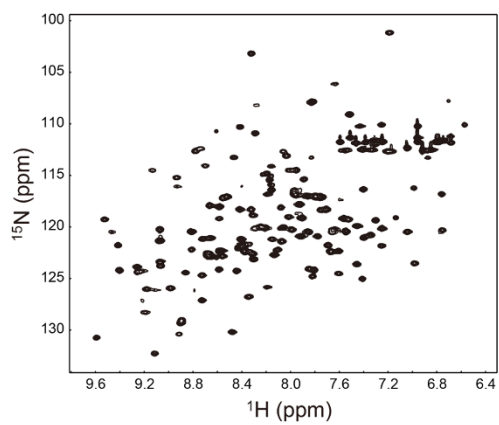


Fig. S2. ^1H - ^{15}N HSQC spectra of H-Ras^{CVLS}•GppNHp (A) and H-Ras^{C(Far)OMe}•GppNHp (B).

A



B

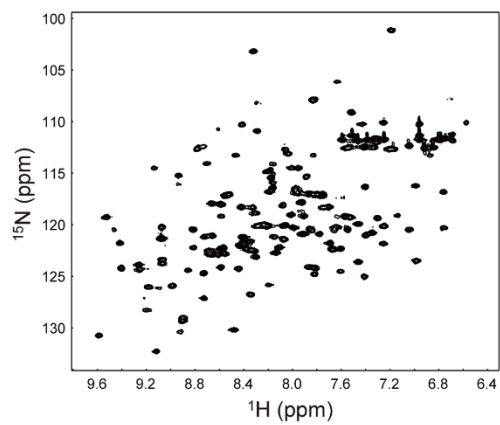


Fig. S3. The signals of Asp54, Ala66 and Met67 exhibiting severe broadenings in the presence of the posttranslational modifications. The ^1H - ^{15}N HSQC spectra of H-Ras^{CVLS}•GppNHp and H-Ras^{C(Far)OMe}•GppNHp are colored by green and red, respectively.

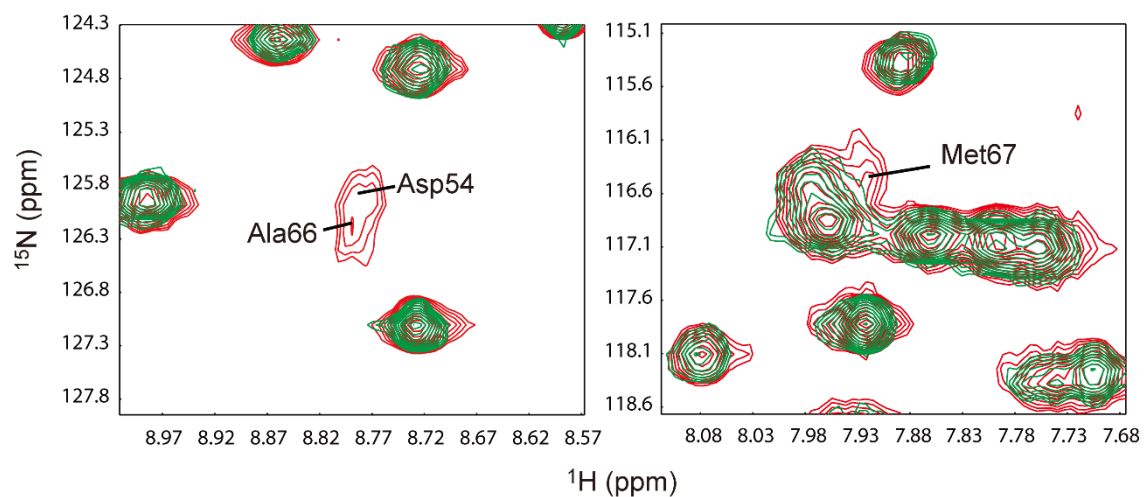


Fig. S4. SPR binding curves of the CVLS (gray) and C(Far)OMe (black) HVR peptides. 6xHis-tagged H-Ras¹⁻¹⁶⁶ was immobilized on an NTA sensor chip. The signals in the blank cell were subtracted as background. The analyte concentrations are labeled on each sensorgram.

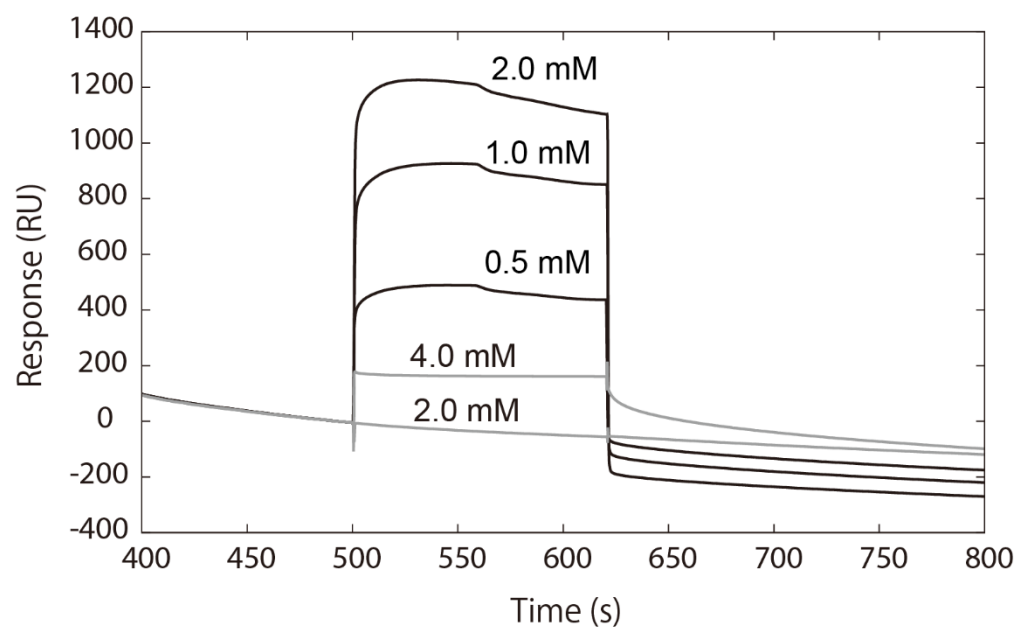


Fig. S5. A model for the compact conformation of modified H-Ras for the cooperative recognition of c-Raf-1-CRD by the activator region and the farnesyl moiety. The colors are identical to those in Fig. S1A. SW I and SW II represent Switch I and Switch II, respectively. Far represents the farnesyl moiety.

